ARTICLE

pH Influence on Performance of Phytic Acid Conversion Coatings on AZ31 Magnesium Alloy in Simulated Body Fluid

Jia Zheng, Sheng-tao Zhang*, Lei Guo, Tang-man Lv, Yang Zhou, Xiao-fang Luo

College of Chemistry and Chemical Engineering, Chongqing University, Chongqing 400030, China

(Dated: Received on April 14, 2014; Accepted on June 16, 2014)

Phytic acid (PA) conversion coating on AZ31 magnesium alloy is prepared by a deposition method. pH influences on the formation process, microstructure and properties of the conversion coating are investigated. Electrochemical tests including polarization curve and electrochemical impedance spectroscopy are used to examine the corrosion resistance, and scanning electron microscopy is used to observe the microstructure. The chemical nature of conversion coating is investigated by energy dispersive spectroscopy. And thermodynamic method is used to analyze the optimum pH. The results show that PA conversion coating can improve the corrosion resistance of AZ31 Mg alloy. The maximum efficiency achieves 89.19% when the AZ31 Mg alloy is treated by PA solution with pH=5. It makes the corrosion potential of sample shift positively about 156 mV and corrosion current density is nearly an order of magnitude less than that of the untreated sample. The thermodynamic analysis shows that the corrosion resistance of PA coatings is affected by not only the concentration of PA ion and Mg^{2+} but also the release rate of hydrogen.

Key words: Phytic acid conversion coating, Corrosion resistance, Corrosion current density, Thermodynamic analysis

I. INTRODUCTION

Magnesium and its alloys have been recently recognized as promising biodegradable orthopedic materials, because of their excellent biocompatibility, low density similar to bone of person, non-toxicity and non-necessity of a second surgery for implant removal. These preferable characters make Mg and its alloys superior to commonly used permanent materials (stainless steel, titanium and cobalt-chromium-based alloys). However, as it is well known Mg and its alloys have such a high corrosion rate in the human body that they will lose mechanical integrity before the fracture has sufficiently fixed. It is important to control the corrosion rates of the Mg-based materials to match the bone healing rate. It is usually accomplished by surface modification of the substrate materials to achieve a desirable corrosion property [1−3].

An inartificial and non-toxic organic big molecule compound, phytic acid (PA), consists of 24 oxygen atoms, 12 hydroxyl groups and 6 phosphate carboxyl groups. The peculiar structure of PA (Fig.1) has powerful chelate capability with many metal ions. In this work, we investigate the reaction of the metal ions on the surface of Mg or its alloys with the active groups of phytic acid to form chelate compounds. The complex compounds deposit on the surface of magnesium alloys to form a chemical conversion coating which could insulate the contact of magnesium alloy base and environmental media. The corrosion resistance of magnesium and its alloys could be improved.

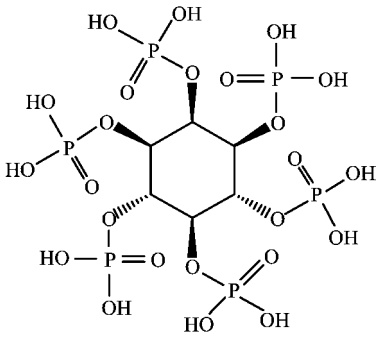

FIG. 1 The structure of PA molecule.

II. EXPERIMENTS

A. Specimen preparation

Commercially available AZ31 Mg alloy was used as substrate material. The AZ31 Mg alloy is constituted of 94.15wt%Mg, 3.01wt%Al, 1.09wt%Zn, 0.37wt%Mn, and 0.002wt%Cu (10 mm×10 mm×10 mm) [4]. Prior

*Author to whom correspondence should be addressed. E-mail: shengtzhang@gmail.com

to the conversion treatment, all samples were polished with grade 1000♯ and 2000♯ carborundum papers and washed with deionized water and ethyl alcohol for 3 min, and then immediately dried in warm flowing air. The samples were treated with the solution containing 4 g/L of PA with different pH values of 2, 4, 5, 6, 7, and 8, at 40 °C for 40 min. The pH values of solution were adjusted with NaOH.

B. Electrochemical test

Electrochemical tests were carried out by using conventional three-electrode system with substrate as working electrode (WE), Pt and saturated calomel electrode (SCE) as counter (CE) and reference electrode (RE), respectively. Simulated body fluid (SBF) solution was used as physiological medium and its compositions include 8.035 g/L NaCl, 0.355 g/L $NaHCO_3$, 0.225 g/L KCl, 0.231 g/L $K_2HPO_4{\cdot}3H_2O$, 0.311 g/L $MgCl_2{\cdot}6H_2O$, 0.292 g/L $CaCl_2$, 39 mL 1.0 mol/L HCl, and 0.072 g/L Na_2SO_4 in 6.118 g/L $(HOCH_2)_3CNH_2$ (Tris). The solution was buffered with $(HOCH_2)_3CNH_2$ (Tris) and 1.0 mol/L HCl to a physiological pH of 7.5 at 25 °C. The SBF was refreshed each day and maintained at the most common body temperature of 36.5±0.5 °C.

The polarization curves were measured in the range of −1.8 V to −1.4 V with a scan rate of 1 mV/s. The EIS tests were performed over the frequency range from 0.02 Hz to 100 kHz with a sinusoidal perturbation of ±5 mV after 50 min of immersion in SBF. All the electrochemical experiments were carried out in SBF at 36.5 °C with the electrochemical system (CHI604d). *Z*-view software has been used for curve fitting of the obtained impedance results.

C. Specimen characterization

The scanning electron microscopy (SEM) micrographs and the energy dispersive X-ray spectroscopy (EDS) used to examine the element compositions of PA conversion coatings were obtained using TESCAN VEGAII.

III. RESULTS AND DISCUSSION

A. Polarization curve test

Polarization curves of AZ31 Mg alloys with and without PA coating in SBF solution are graphed in Fig.2. The important parameters such as corrosion potential E_{corr} and corrosion current density I_{corr} are generated directly from the polarization curves through cathodic Tafel extrapolation. E_{corr} and I_{corr} are listed in Table I.

It can be observed from Table I that all the coated samples show higher E_{corr} than uncoated AZ31 irrespective of pH. This suggests that PA coated samples are less reactive to SBF as compared to uncoated AZ31 alloys. The E_{corr} of the sample treated with the solution of pH=5 is the highest with −1.498 V, which is 156 mV higher than uncoated AZ31 alloy. However, PA conversion coatings treated with solution of pH=2, 4, 6, 7, 8 show lower corrosion potential from −1.606 V to −1.505 V, which reveals that Mg alloy AZ31 treated with PA of pH=5 has the best corrosion resistance in SBF.

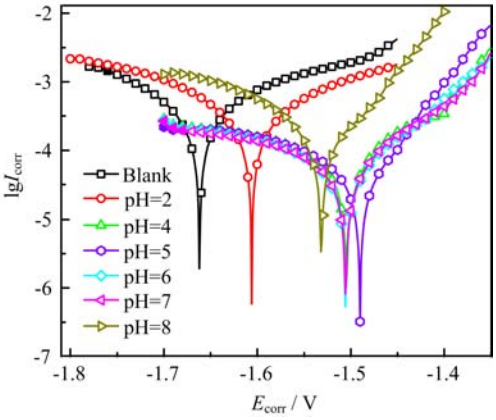

FIG. 2 Polarization curves of AZ31 Mg alloys with and without PA coating in SBF solution.

TABLE I The electrochemical corrosion data related to polarization curves of different coatings.

pH	E_{corr}	I_{corr}	β_c	β_a	η/%
Blank	−1.654	538.4	5.437	4.487	
2	−1.606	418.9	5.398	5.244	22.19
4	−1.505	78.45	3.105	7.671	85.43
5	−1.498	58.21	3.349	16.11	89.19
6	−1.506	62.67	5.104	9.777	88.36
7	−1.506	66.37	4.204	8.598	87.67
8	−1.534	244.5	5.467	17.39	54.59

Note: E_{corr} in V (*vs.* SCE), I_{corr} in μA/cm^2 (*vs.* SCE), β_c and β_a are slope of anode and cathod polarization curve, in mV/°.

I_{corr} can also be used to judge the corrosion resistance of Mg alloy. The less I_{corr} is, the better E_{corr} is. It can be seen from the data presented in Table I that the I_{corr} of all the coated samples are much lower than that of uncoated AZ31 alloy, indicating that the corrosion resistance has been improved through the treatment in the solution containing PA. Especially, I_{corr} decreases to 58.21 μA/cm^2 after being treated with PA of pH=5 which is the lowest in all the samples and the efficiency achieves 89.19% measured by Eq.(1) [6−9].

$$\eta = \frac{I^0_{corr} - I^i_{corr}}{I^0_{corr}} \times 100\% \quad (1)$$

DOI:10.1063/1674-0068/27/05/535-540

where I^0_{corr} is corrosion current density for uncoated sample, I^i_{corr} is corrosion current density for coated sample by PA solution with different pH. These results confirm that the coated alloy treated with solution of pH=5 can offer enhanced corrosion resistance in SBF. And it can be seen that the polarization curves of the AZ31 magnesium alloys treated with PA solutions of pH=4, 6, and 7 overlap with each other. The I_{corr} is about 65 μA/cm^2, which is a little higher than the AZ31 Mg alloy treated with the PA solution of pH=5. However, the corrosion resistance of samples treated with PA of pH=2 and 8 has been rarely improved [10−12].

B. Electrochemical impedance spectroscopy

The EIS results obtained at the open circuit potential for uncoated and PA coated AZ31 Mg alloy after immersion for 50 min in SBF are presented in Fig.3. The uncoated and coated with PA of pH=2, 4, 7, and 8 exhibit three-time constants behavior, *i.e.* two capative loops and one inductance loop, which can be seen from the Bode plot (Fig.3(a)). The first-time constant (capacitive loop) appearing in the high frequency region (10^4−10^2 Hz) is attributed to the charge transfer reaction in the electric double layer formed at the interface between the surface of Mg alloy and SBF medium. The capacitive loop appearing at the middle frequency (10−0.1 Hz) region is related to the mass transport in solid phase, *i.e.* diffusion of ions from the electrolyte to the metal. The inductive loop appearing at the low frequency region (0.1−0.02 Hz) could be attributed to the adsorption of corrosive ions present in the SBF [13]. However, there are only two-time constants without the inductance loop when the pH=5 and 6, which can be attributed to the disappearance of the adsorbed corrosive ions from the SBF solution. The value of the impedance modulus at the low frequency (0.1−0.02 Hz) is a key parameter, which could be used to compare the protection provided by uncoated and PA coated AZ31 Mg against corrosion in SBF solution. It can be found that the pH=5 exhibits about one order of increment in the impedance value than that of the uncoated alloy.

The Nyquist plot is given in Fig.3(b). The most important parameters in the Nyquist plot is the diameter of semicircle, which indicates resistance. The diameters of the capacitive loops at high frequency and medium frequency correspond to the charge transfer resistance and surface film resistance for mass transfer, respectively. It is obvious that the diameters of coated AZ31 Mg alloy are larger than the uncoated sample [14, 15]. And it increases as the concentration of H^+ decreases before pH=5, however the diameter starts declining above pH=5. So the diameters of coated AZ31 Mg alloy treated with PA of pH=5 are the largest for both semicircles. Hence it could be attributed that the coated AZ31 Mg alloy treated with PA of pH=5 provides resistance to the ingress of aggressive ions through the film.

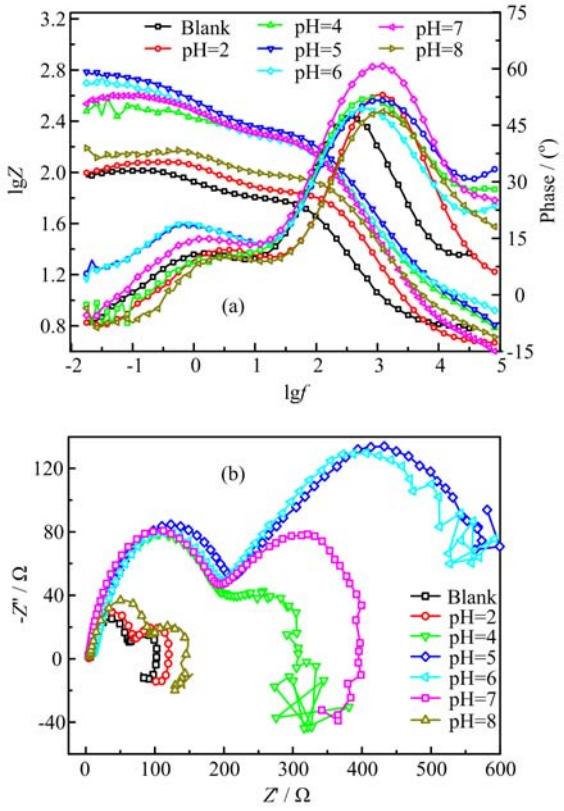

FIG. 3 Bode plots (a) and Nyquist (b) of uncoated and PA coated AZ31 Mg alloy in SBF solution after 50 min immersion at different pH. Z is resistance, Z' is the real part of resistance, Z'' is the imaginary part of resistance, f is the scanning frequency of EIS, and phase is the relationship of potential or current and frequency.

In order to acquire more information about the measured EIS results, the curve fitting analysis is performed using Z-view software. The equivalent circuits are presented in Fig.4 and the fitting results are shown in Table II. The error of the non-linear least square fitting of the experimental data is less than 10% and agrees with the experimental data. Various equivalent circuit elements are used to construct the equivalent circuits including are solution resistance R_s, constant phase element of double layer and film (CPE_{ct} and CPE_f), charge transfer and film resistance (R_{ct} and R_f), inductive resistance and inductance related to adsorbed intermediate during corrosion (R_L and L). The increasing trend in the R_{ct} and R_f value was observed with increasing pH of PA solution up to 5, however the value started declining above 5. The R_{ct} of 236.1 Ω from the sample treated with PA solution of pH=5 is the largest among all the samples, and its efficiency is 74.59% measured by Eq.(2), which is consistent with the result of polarization test.

$$\eta = \frac{R^i_{ct} - R^0_{ct}}{R^i_{ct}} \times 100\% \quad (2)$$

DOI:10.1063/1674-0068/27/05/535-540

TABLE II Parameters of equivalent circuit for coated and uncoated samples in SBF solution.

pH	$R_s/\Omega\cdot cm^2$	$R_{ct}/\Omega\cdot cm^2$	CPE_{ct}		$R_f/\Omega\cdot cm^2$	CPE_f		$R_L/\Omega\cdot cm^2$	$L/H\cdot cm^2$	$\eta/\%$
			$Y_{ct}/(\mu F/cm^2)$	n_{ct}		$Y_f/(\mu F/cm^2)$	n_f			
Blank	6.02	60.0	28.83	0.85	37.52	2330	0.91	15.59	192.5	
2	4.57	68.1	22.29	0.88	49.05	2050	0.89		29.67	11.8
4	5.70	227.4	48.10	0.72	83.71	2310	0.97		1127	73.6
5	5.45	236.1	42.49	0.71	371.5	1400	0.75			74.5
6	8.27	193.9	42.70	0.74	328.8	1590	0.75			69.0
7	3.959	205.1	26.45	0.81	186.7	1220	0.86		4547	70.7
8	4.956	100.8	41.84	0.76	37.39	1500	0.92		240.2	40.5

Note: Y_{ct} is one parameter of interface capacitance, Y_f is one parameter of film capacitance, and n_f is one parameter of capacitance, it is a index.

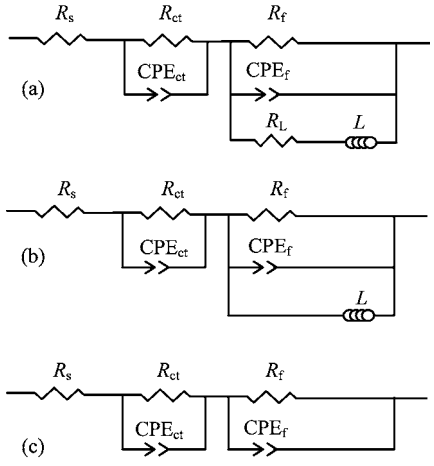

FIG. 4 Electrical equivalent circuits of (a) AZ31 Mg alloy, (b) PA with pH=2, 4, 7, and 8 coated AZ31 Mg alloy, and (c) PA with pH=5 and 6 coated AZ31 Mg alloy in simulated body fluid. The equivalent circuits include are solution resistance R_s, film (CPE_{ct} and CPE_f), film resistance (R_{ct} and R_f), inductive resistance (R_L), and inductance related to adsorbed intermediate during corrosion (L).

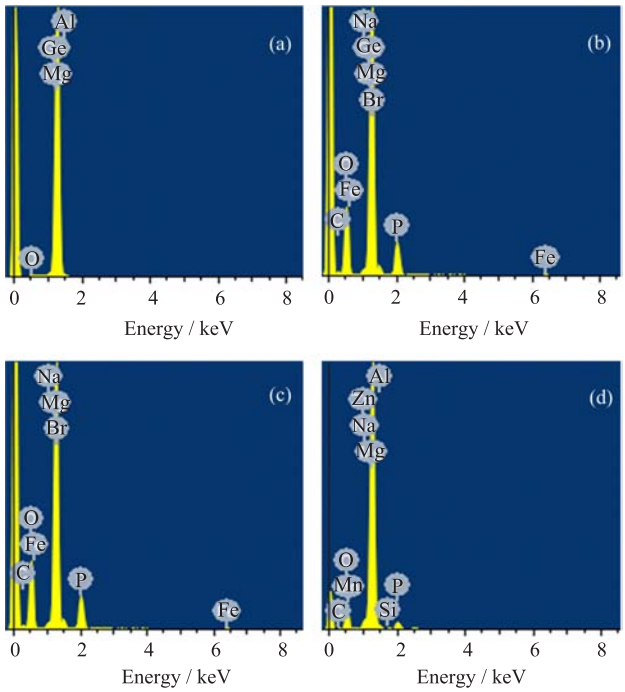

FIG. 5 EDS images of uncoated and PA coated AZ31 Mg alloy. (a) Blank, (b) pH=2, (c) pH=5, and (d) pH=8.

where R_{ct}^i is charge transfer resistance of coated samples by PA solution with different pH, R_{ct}^0 is charge transfer resistance of uncoated sample. It can be seen that the values from pH=2 and 8 are close to the blank which means the corrosion resistance of them are rarely improved, probably the coatings are incomplete, and the attack by corroding ions is more [16−19].

C. Thermodynamic analysis

Figure 5 shows the EDS test results of PA conversion coating on AZ31 Mg alloy. As shown in Fig.5, the conversion coating mainly consists of Mg, O, P, and C when the pH of PA solution is 2 and 5; however, when the pH is 8, Al appears, which may come from the substrate. Because Mg is more active than Al, Mg is anode while Al is cathode in the reaction. Hence it can be concluded that the conversion coating is without Al^{3+}. Table III shows the ionization of PA.

When pH<5, the PA ionizes as follows:

$$H_{12}Phy \Leftrightarrow 6H^+ + H_6Phy^{6-} \tag{3}$$

When pH=7.5−8.0, the PA ionizes as follows:

$$H_{12}Phy \Leftrightarrow 8H^+ + H_4Phy^{8-} \tag{4}$$

The reactions of forming PA conversion coating occurs [19]:

DOI:10.1063/1674-0068/27/05/535-540

TABLE III The ionization of PA and ionized constant K.

pH	The number of ionized proton	K
<5	Six strong ionized protons	1.8
7.5−8.0	Two weakly ionized protons	6.3
>10	Four very weakly ionized protons	9.7

TABLE IV The electrochemical corrosion data related to polarization curves of different coatings in PA solution.

pH	E_{corr}/V	I_{corr}/(μA/cm^2)	β_c/(V/°)	β_a/(V/°)
2	−1.676	991.9	4.998	4.382
5	−1.403	123.2	4.453	5.095
8	−1.320	70.32	5.542	4.245

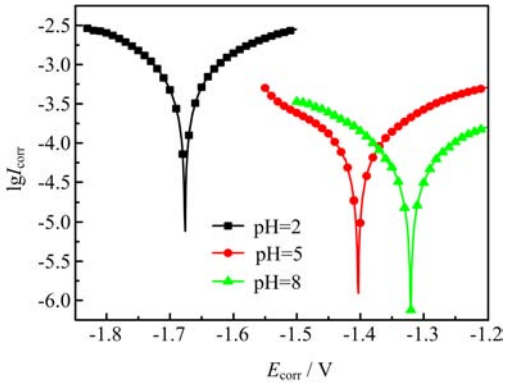

FIG. 6 Polarization curves of AZ31 Mg alloys in PA solution after 40 min immersing.

$$\mathrm{Mg}-2\mathrm{e}^- \rightarrow \mathrm{Mg}^{2+} \quad (5)$$

$$\mathrm{H_6Phy}^{6-}+\mathrm{Mg}^{2+}+4\mathrm{Na}^+ \Leftrightarrow \mathrm{Na_4\,[MgH_6Phy]}\downarrow \quad (6)$$

$$\mathrm{H_4Phy}^{8-}+\mathrm{Mg}^{2+}+6\mathrm{Na}^+ \Leftrightarrow \mathrm{Na_6\,[MgH_4Phy]}\downarrow \quad (7)$$

$$v_{\mathrm{pH=2}} = k\alpha_{\mathrm{H_6Phy^{6-}}}\alpha_{\mathrm{Mg^{2+}}} \quad (8)$$

$$v_{\mathrm{pH=5}} = k\alpha_{\mathrm{H_6Phy^{6-}}}\alpha_{\mathrm{Mg^{2+}}} \quad (9)$$

$$v_{\mathrm{pH=8}} = k\alpha_{\mathrm{H_4Phy^{8-}}}\alpha_{\mathrm{Mg^{2+}}} \quad (10)$$

where v is the velocity of chelating, k is reaction rate constant, α is activity.

$\alpha_{\mathrm{H_6Phy^{6-}}}$ and $\alpha_{\mathrm{H_6Phy^{8-}}}$ are calculated based on Eq.(3) and Eq.(4),

$$M = \alpha_{\mathrm{H^+}}{}^3 + \alpha_{\mathrm{H^+}}{}^2K_{a1} + \alpha_{\mathrm{H^+}}K_{a1}K_{a2} + K_{a1}K_{a2}K_{a3} \quad (11)$$

$$\alpha_{\mathrm{H_{12}Phy}} = \frac{1}{M}\alpha_{\mathrm{H^+}}{}^3 \times 100\% \quad (12)$$

$$\alpha_{\mathrm{H_6Phy^{6-}}} = \frac{1}{M}\alpha_{\mathrm{H^+}}{}^2K_{a1} \times 100\% \quad (13)$$

$$\alpha_{\mathrm{H_4Phy^{8-}}} = \frac{1}{M}\alpha_{\mathrm{H^+}}K_{a1}K_{a2} \times 100\% \quad (14)$$

$$\alpha_{\mathrm{Phy^{12-}}} = \frac{1}{M}K_{a1}K_{a2}K_{a3} \times 100\% \quad (15)$$

$\alpha_{\mathrm{Mg^{2+}}}$ is calculated based on Eq.(5)

$$j = \frac{Q}{t} = \frac{n_{\mathrm{e^-}}N_{\mathrm{A}}\mathrm{e}^-}{t} \quad (16)$$

$$n_{\mathrm{e^-}} = \frac{tj}{N_{\mathrm{A}}\mathrm{e}^-} \quad (17)$$

$$\alpha_{\mathrm{Mg^{2+}}} = \frac{n_{\mathrm{e^-}}}{2} = \frac{tj}{2N_{\mathrm{A}}\mathrm{e}^-} \quad (18)$$

where j is corrosion current, t is time, N_{A} is constant, Q is electricity. Taking the results into Eqs. (8), (9), and (10), the final results are as Eqs.(19), (20), and (21),

$$v_{\mathrm{pH=2}} = k\alpha_{\mathrm{H_6Phy^{6-}}}\frac{tj_{\mathrm{pH=2}}}{2N_{\mathrm{A}}\mathrm{e}^-} \quad (19)$$

$$v_{\mathrm{pH=5}} = k\alpha_{\mathrm{H_6Phy^{6-}}}\frac{tj_{\mathrm{pH=5}}}{2N_{\mathrm{A}}\mathrm{e}^-} \quad (20)$$

$$v_{\mathrm{pH=8}} = k\alpha_{\mathrm{H_4Phy^{8-}}}\frac{tj_{\mathrm{pH=8}}}{2N_{\mathrm{A}}\mathrm{e}^-} \quad (21)$$

here k, t, N_{A}, and e^- are equal, so only $\alpha_{\mathrm{H_6Phy^{6-}}}$, $\alpha_{\mathrm{H_4Phy^{8-}}}$, and j are the parameters that have effect on v, and j is equal to I_{corr} listed in Table IV from the polarization curves through cathodic Tafel extrapolation as shown in Fig.6.

N_A=6.023×10^{23}, e^-=1.6×10^{-19} C, $c_{\mathrm{H_{12}Phy}}$=4 g/L= 6.06×10^{-3} mol/L, t=2400 s, K_{a1}=10$^{-1.8}$, K_{a2}=10$^{-6.3}$, K_{a3}=10$^{-9.7}$.

(i) pH=2, $\alpha_{\mathrm{H^+}}$=10^{-2}, j=991.9 μA/cm^2. $\alpha_{\mathrm{H_6Phy^{6-}}}$= 61.31%=3.715×10^3 mol/L. $v_{\mathrm{pH=2}}$=1.236×10^{-8}k.

(ii) pH=5, $\alpha_{\mathrm{H^+}}$=10^{-5}, j=123.2 μA/cm^2. $\alpha_{\mathrm{H_6Phy^{6-}}}$= 95.17%=5.767×10^3 mol/L. $v_{\mathrm{pH=2}}$=8.85×10^{-9}k.

(iii) pH=8, $\alpha_{\mathrm{H^+}}$=10^{-8}, j=70.32 μA/cm^2. $\alpha_{\mathrm{H_6Phy^{6-}}}$= 96.16%=5.827×10^3 mol/L. $v_{\mathrm{pH=2}}$=5.1×10^{-9}k.

From the results shown above, $v_{\mathrm{pH=2}}$ is larger compared to $v_{\mathrm{pH=5}}$, $v_{\mathrm{pH=8}}$, which do not accord with the results achieved from Polarization curve test. The reason may be that the effects of the release of hydrogen on the conversion coatings are ignored in the thermodynamic analysis. And it can be seen from the SEM that many cracks appear when pH=2 which are caused by the release of hydrogen [20−25].

D. Scanning electron microscopic studies

Figure 7 shows the scanning electron microscopic (SEM) images of the PA coatings on the AZ31 Mg alloys treated in different pH PA solutions with a concentration of 4 g/L for 40 min immersing time. For PA solutions of pH=5, the microstructure of the coating is continuous and compact compared to the blank. But

DOI:10.1063/1674-0068/27/05/535-540

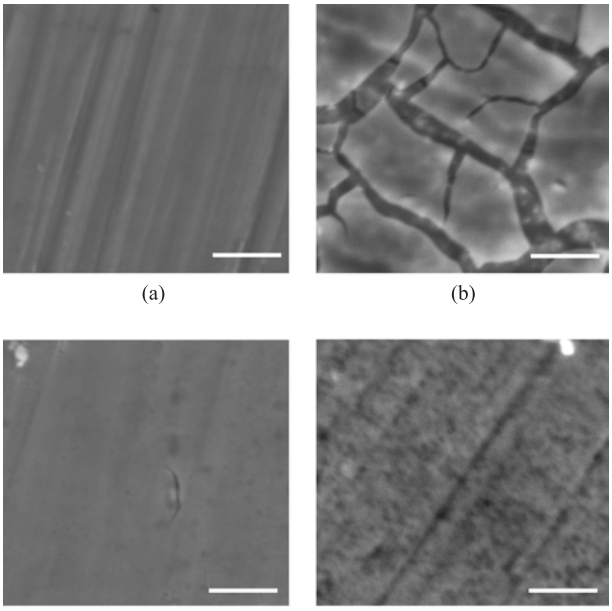

FIG. 7 SEM images of the PA coatings on the AZ31 Mg alloys obtained from different pH. (a) blank, (b) pH=2, (c) pH=5, and (d) pH=8. The scale bars are 100 μm.

there are some micro-cracks on the coatings when the pH=2. And the coating of pH=8 is too thin to cover the surface of Mg alloy, which is in agreement with the results of polarization and EIS tests.

IV. CONCLUSION

pH of PA solution has an important effect on the corrosion resistance of PA coatings on AZ31 Mg alloy. The conversion coating can effectively improve its corrosion resistance under appropriate conditions. The best conversion coating can be obtained in PA solution of pH=5, it could make the corrosion potential $E_{\rm corr}$ shift positively about 156 mV and $I_{\rm corr}$ is nearly an order of magnitude less. The thermodynamic analysis shows that the corrosion resistance of PA coatings is affected by not only the concentration of PA ion and Mg^{2+}, but also the release rate of hydrogen. Though the velocity of producing PA coating is larger when pH=2, the release rate of hydrogen is also the largest. So the corrosion resistance of PA coatings when pH=5 is the best.

V. ACKNOWLEDGMENTS

This work was supported by the National Natural Science Foundation of China (No.21376282).

[1] Y. H. Gu, C. F. Chen, S. Bandopadhyay, C. Y. Ning, Y. J. Zhang, and Y. J. Guo, Appl. Surf. Sci. **258**, 6116 (2012).
[2] S. Shadanbaz and G. J. Dias, Acta. Biomater. **8**, 20 (2012).
[3] M. P. Staiger and A. M. Pietak, Biomaterials **27**, 1728 (2006).
[4] L. L. Gao, C. H. Zhang, M. L. Zhang, X. M. Huang, and X. Jiang, J. Alloys. Compd. **485**, 789 (2009).
[5] T. Kokubo and H. Takadama, Biomaterials **27**, 2907 (2006).
[6] J. Y. Hu, D. Z. Zeng, Z. Zhang, T. H. Shi, G. L. Song, and X. P. Guo, Corros. Sci. **74**, 35 (2013).
[7] R. F. Zhang, S. F. Zhang, and S. W. Duo, Appl. Surf. Sci. **255**, 7893 (2009).
[8] S. Y. Shen, Y. Zuo, and X. H. Zhao, Corros. Sci. **76**, 275 (2013).
[9] X. H. Guo, K. Q. Du, Q. Z. Guo, Y. Wang, R. Wang, and F. H. Wang, Corros. Sci. **76**, 129 (2013).
[10] R. K. Gupta, K. Mensah-Darkwa, and D. Kumar, Mater. Sci. Technol. **29**, 180 (2013).
[11] Y. W. Song and D. Y. Shan, Mater. Lett. **62**, 3276 (2008).
[12] C. L. Wen and S. K. Guan, Appl. Surf. Sci. **255**, 6433 (2009).
[13] A. Srinivasan, P. Ranjani, and N. Rajendran, Electrochim. Acta **88**, 310 (2013).
[14] M. Jamesh, S. Kumar, and T. S. N. S. Narayanan, Corros. Sci. **53**, 645 (2011).
[15] J. R. Liu, Y. N. Guo, and W. D. Huang, Surf. Coat. Technol. **201**, 1536 (2006).
[16] X. F. Cui, Y. Li, Y. Li, F. H. Wang, G. Jin, and M. H. Ding, Mater. Chem. Phys. **111**, 503 (2008).
[17] Y. W. Song and D. Y. Shan, Mater. Lett. **62**, 3276 (2008).
[18] S. X. Zhang and X. N. Zhang, Acta Biomater. **6**, 626 (2010).
[19] F. S. Pan, X. Yang, and D. F. Zhang, Appl. Surf. Sci. **255**, 8363 (2009).
[20] X. F. Cui, Y. Li, Q. F. Li, G. Jin, M. H. Ding, and F. H. Wang, Appl. Surf. Sci. **255**, 2098 (2008).
[21] J. Chen, Y. W. Song, D. Y. Shan, and E. H. Han, Corros. Sci. **74**, 130 (2013).
[22] T. T. Tran, R. H. Kaul, S. Dalagaard, and S. K. Yu, Anal. Biochem. **410**, 177 (2011).
[23] Y. H. Gu, C. F. Chen, S. K. Bandopadhyay, C. Y. Ning, and Y. J. Zhang, Appl. Surf. Sci. **258**, 6116 (2012).
[24] X. Y. Ye, Y. Dou, G. H. Xu, K. Huang, M. G. Ren, and X. X. Wang, Appl. Surf. Sci. **259**, 799 (2012).
[25] N. N. Aung and W. Zhou, Corros. Sci. **52**, 589 (2010).

DOI:10.1063/1674-0068/27/05/535-540